A recipe for stringy naturalness

Dakotah Martinez

1 Stringy naturalness as a probability measure in the landscape

Stringy naturalness may be viewed as a measure of the relative abundance of vacua satisfying some set of criteria, such as the ABDS condition, relative to all "viable" vacua. By "viable", we mean that a select set of alternative criteria are satisfied, such as proper EWSB and absence of CCB minima (such as negative squared masses in squarks or sleptons). Here, stringy naturalness is defined as the following [1]:

Stringy naturalness: *The value of an observable $\mathcal{O}_2$ is more stringy natural than a value $\mathcal{O}_1$ if more phenomenologically viable vacua lead to $\mathcal{O}_2$ than to $\mathcal{O}_1$.*

In particular, choosing the mass of the Z boson and its relation to the ABDS window as a selection criterion for vacua satisfying the atomic principle, then we can say:

If more vacua lead to the ABDS window in scenario **A** than in scenario **B**, then scenario **A** is considered more *stringy natural* than scenario **B**.

In regards to "scenarios", one can compare different realizations of supersymmetry on the landscape, such as comparing high-scale SUSY against radiative natural SUSY (RNS), or even against non-supersymmetric models like the Standard Model. However, this idea is very broad in and of itself. In practice, a researcher may just have data on a single possible vacuum where m_Z is tuned to 91.1876 GeV, such as in an SLHA file for a supersymmetric spectrum generated by a spectrum generator. For this reason, it is necessary to create a stringy naturalness measure that can evaluate the relative abundance of ABDS-compliant vacua "surrounding" some initial vacuum in the landscape, relative to the total number of EWSB-compliant and no-CCB vacua. These are the efforts presented here.

In [2], we determined an approximate relative probability, P_μ, based on the Higgsino (or Higgs) mass parameter μ^{PU} within some pocket universe of the landscape with variable m_Z. This effectively offered a comparison standard between scenarios, comparing the "width" of the ABDS window in these scenarios by evaluating m_Z^{PU} from the relevant weak-scale parameters and μ^{PU} with the Higgs minimization conditions (or weak-scale mass conditions in the Standard Model) in the following models:

- Radiative natural SUSY,
- mSUGRA/CMSSM,
- Split SUSY,
- Mini-split SUSY,
- Spread SUSY,
- High-scale SUSY,
- PeV SUSY,

- the Standard Model.

The evaluations to obtain this measure P_μ can be expressed as the following integral. Let the lower edge of the ABDS window lie at $m_Z^{\rm OU}/2 = 45.6$ GeV, and the upper edge lie at $4m_Z^{\rm OU} = 364.8$ GeV. These values are obtained by leaving other variables (such as soft terms) fixed at some predetermined value, then scanning over $\mu^{\rm PU}$ and solving for $m_Z^{\rm PU}$. The $\mu^{\rm PU}$ term is distributed on the landscape in a fashion such that mu is uniformly distributed over the decades, i.e., the probability distribution of μ^{PU} is

$$f_\mu \sim \frac{1}{\ln(10)\mu^{\rm PU}} \tag{1}$$

Then the unnormalized probability (unnormalized CDF) associated with vacua containing $\mu^{\rm PU}$ values leading to the ABDS window allow us to approximately compare different landscape vacuum scenarios as

$$\begin{aligned} P_\mu &= \int_{\mu^{\rm PU}(\rm min)}^{\mu^{\rm PU}(\rm max)} f_\mu \; d\mu^{\rm PU} \\ &= \log_{10}\left(\frac{\mu^{\rm PU}(\rm max)}{\mu^{\rm PU}(\rm min)}\right). \end{aligned} \tag{2}$$

Clearly, "wider" ABDS windows (as in RNS) will lead to many more vacua that are ABDS-compliant, relative to "narrower" ABDS windows (as in the Standard Model, up to $\sim 10^{26}$ times smaller of a probability relative to RNS). Two primary "incompleteness" issues arise here, however:

1. The probability measure here is unnormalized and only can effectively compare different, pre-simulated scenarios. Without a proper normalization factor, an incomplete picture may be presented.

2. There are other parameters potentially distributed on the landscape. For example, soft-SUSY-breaking (SSB) terms could be distributed on the landscape according to a power-law distribution, based on the number of F- and D-type SUSY breaking fields present in the theory [3]. A more complete probability measure would incorporate the statistical contributions of these terms to the relative population of the ABDS window.

Since we understand the statistical distributions of soft terms on the landscape, and we couple the ABDS window criterion with other criteria such as proper EWSB and absence of CCB minima, we can simultaneously address both of these issues. Moreover, coupling these ideas with a specialized hit-or-miss Monte Carlo simulation to refine our results, an algorithm will be constructed below to permit a "point-by-point" evaluation of stringy naturalness.

2 Requirements for a stringy naturalness measure

If one were to try and evaluate stringy naturalness in a reliable manner more rigorously than simply "counting dots" from a multiverse simulation, there are a few key details that *must* be included in the evaluation.

1. One must account for the probability distributions of terms (e.g., soft terms distributed as power law based on number of D and F SUSY-breaking fields) on the string landscape;

2. One must incorporate a method for *counting* the number of vacua leading to some observable, as given by the definition of stringy naturalness;

3. Since on the string landscape, m_Z is variable, one can use a set of selection criteria for "valid" vacua as:

(a) The Z boson mass lies within the ABDS window, as determined by the weak-scale Higgs minimization conditions:

$$\frac{m_Z^2}{2} = \frac{m_{H_d}^2 + \Sigma_d - (m_{H_u}^2 + \Sigma_u)\tan^2(\beta)}{\tan^2(\beta) - 1} - \mu^2 \tag{3}$$

$$\sin(2\beta) = \frac{2b}{m_{H_u}^2 + \Sigma_u + m_{H_d}^2 + \Sigma_d + 2\mu^2}. \tag{4}$$

$\Sigma_{u,d}$ are radiative loop corrections to these equations. The ABDS requirement may be relaxed if we are finding a total count of "viable" vacua.

(b) There are no CCB minima.

(c) The electroweak symmetry is satisfactorily broken, i.e., when the following weak-scale conditions are true:

$$2b < 2\mu^2 + m_{H_u}^2 + \Sigma_u + m_{H_d}^2 + \Sigma_d, \tag{5}$$

$$b^2 > \left(\mu^2 + m_{H_u}^2 + \Sigma_u\right)\left(\mu^2 + m_{H_d}^2 + \Sigma_d\right). \tag{6}$$

(d) It will be otherwise assumed that the SM fermion masses do not vary from vacuum to vacuum, i.e., $m_t = 173.2$ GeV, $m_b = 4.25$ GeV, $m_\tau = 1.777$ GeV, etc.

4. One should compare the number of vacua lying within the ABDS window to some total number of vacua with weak scales also perhaps out of the ABDS window, but with no CCB minima and valid EWSB.

Next, we construct two algorithms used to accomplish these requirements and produce a measure for evaluating stringy naturalness on a point-by-point basis.

3 Numerical precision and statistical considerations

Depending on the level of statistical rigor we would like to apply to this probability measure, different approximations of the stringy naturalness value can be employed. The level of accuracy of these approximations are directly proportional to their levels of robustness for the corresponding statistical analyses of the landscape, and hence, the level of computational complexity. In brief, we present both an approximate expression (à la P_μ) and a more robust and specialized Monte-Carlo simulation algorithm for computing the probability of an ABDS-compliant vacuum randomly emerging from the landscape. The landscape is assumed to be parameterized by the Minimally Supersymmetric Standard Model (MSSM) parameter space, in some local neighborhood surrounding one user-specified possible vacuum with the MSSM and Standard Model (SM) (with potentially different Z boson mass) as its low-energy effective field theories (EFTs). The specific requirements are outlined in the previous section.

Many supersymmetric spectrum generators today (e.g., SoftSUSY, Isajet/Isasugra, SPheno, etc.) can provide predictions of the MSSM that are potentially testable at a collider. Often, the user is able to save their results to a standardized format, the SUSY Les Houches Accord (SLHA) [4, 5]. From this format, one can compute various naturalness measures such as the electroweak naturalness measure Δ_{EW}, the high-scale naturalness measure Δ_{HS}, and the Barbieri-Giudice naturalness measure Δ_{BG}. These can all be calculated from a user-submitted SLHA-format file, from the user's choice of spectrum generator, using the program DEW4SLHA, developed by D. Martinez [6]. In a similar sense, we have developed a program to compute a proposed stringy naturalness measure. In an approximate form, we can write this stringy naturalness measure as an analytic expression. In its more robust form, it is instead expressed as an algorithm for effectively counting vacua.

However, before introducing these expressions and algorithms, we must ensure we have a concrete method for counting vacua. Included in this is the requirement of understanding the parameter space in which we are computing probabilities. For this reason, we parameterize some "friendly" neighborhood of the landscape surrounding an initial vacuum with the MSSM parameters. The MSSM in itself contains a vast parameter space, though, so we specifically restrict ourselves to the *real*-valued MSSM, but still maintain some generality by relaxing universality conditions beyond even those in the pMSSM-19 by allowing non-universal first and second generation GUT-scale soft trilinear couplings and masses. We also assume the relevant gauge-eigenstate mass matrices are diagonal. In our proposed parameter space here, we assume there are 30 fundamental soft supersymmetry-breaking (SSB) parameters (15 SSB squark/slepton masses, two SSB Higgs masses, nine SSB trilinear couplings, three SSB gaugino masses, and one SSB bilinear parameter) along with one supersymmetry-conserving parameter, μ, which is important for weak-scale physics. This full parameter space can then be written as the set:

$$\left\{\begin{array}{c} m^2_{\widetilde{Q}_1}, m^2_{\widetilde{U}_1}, m^2_{\widetilde{D}_1}, m^2_{\widetilde{L}_1}, m^2_{\widetilde{E}_1}, m^2_{\widetilde{Q}_2}, m^2_{\widetilde{U}_2}, m^2_{\widetilde{D}_2}, m^2_{\widetilde{L}_2}, m^2_{\widetilde{E}_2}, \\ m^2_{\widetilde{Q}_3}, m^2_{\widetilde{U}_3}, m^2_{\widetilde{D}_3}, m^2_{\widetilde{L}_3}, m^2_{\widetilde{E}_3}, a_t, a_c, a_u, a_b, a_s, a_d, a_\tau, a_\mu, a_e, \\ m^2_{H_u}, m^2_{H_d}, M_1, M_2, M_3, b, \mu \end{array}\right\}.$$

Vacua in the landscape can be selected for analysis according to a well-defined set of selection criteria, which we will denote generally here as an indicator function θ. θ is defined as

$$\theta = \theta(\text{conditions}) = \begin{cases} 1 & \text{if conditions are true,} \\ 0 & \text{otherwise.} \end{cases} \tag{7}$$

According to Douglas and others [3], these soft-supersymmetry breaking terms may be distributed in the string landscape according to the numbers n_F and n_D of F- and D-type SUSY breaking fields, where these fields may lie in some hidden sector or potentially within a more UV-complete theory that breaks down to the MSSM as an EFT somewhere below M_{Pl}, the reduced Planck scale. This can be expressed approximately as a density of vacua, scaled by the power law distribution provided by the number of SUSY-breaking fields:

$$\begin{aligned} dN_{\text{vac, soft}} &\sim f_{\text{SUSY}}\left(m_{\text{soft}}\right) \cdot \theta \cdot dm_{\text{soft}} \\ &\sim m_{\text{soft}}^{2n_F+n_D-1} \cdot \theta \cdot dm_{\text{soft}}, \end{aligned} \tag{8}$$

To be consistent with the distribution of Standard Model fermion masses, then we suppose that the distribution of μ on the landscape can be expressed as a $\log_{10}$-uniform distribution (simultaneously allowing for $\mu < 0$ solutions):

$$\begin{aligned} dN_{\text{vac, }\mu} &\sim f_\mu(\mu) \cdot \theta \cdot \ d\mu \\ &\sim \frac{\theta}{\log(10)|\mu|} \cdot d\mu. \end{aligned} \tag{9}$$

Note that integrating Eq. (9) then leads to the expression for P_μ in Eq. (2). A similar idea, together with certain assumptions, allows us to come up with an explicit, but approximate evaluation of the desired ABDS probability.

3.1 P_μ-esque expression

For deriving the analytic but approximate expression, we start with some assumptions on our statistical distributions. First, we assume each of the 30 specified soft terms and μ are all distributed independently of one another. In the bulk of the neighborhood of the landscape surrounding the user-supplied vacuum where we wish to evaluate stringy naturalness, this will be approximately true. However, for a given set of selection criteria θ, this independence assumption causes our selection criteria to select a hyperrectangular region in this 31-dimensional parameter space (30 dimensions of soft parameters, one dimension for the μ parameter). In particular, the independence assumption specifies that the *boundaries* of the region defined by our indicator function θ are *rectangular*. In general, this is not the case. This is particularly important due to the high dimensionality of this parameter space and the indicated region: it is a well known fact in geometry that in higher dimensional shapes and regions, the significant majority of the hypervolume of that shape lies near its boundary. In the context of the landscape, this would mean that the majority of vacua geometrically live near the boundaries of our selected region. This distribution of vacua is then shifted further by the probability distributions of our parameters.

Since we are counting vacua in the string landscape by parameterizing them in this high-dimensional parameter space, counting ABDS-compliant vacua is tantamount to finding a weighted hypervolume of the region of parameter space containing these ABDS-compliant vacua. Due to the high dimensionality, subtle variations in region boundaries can result in significant deviations in the evaluation of this weighted hypervolume, where the weights come from the known probability densities of each parameter. When the boundary of a statistically indicated region (such as the one indicated by θ) is nonrectangular, this implies that the boundary is inducing some correlations between the random variables at that boundary. So, despite the relative independence of statistical distributions in the bulk of the indicated region of parameter space, potentially important correlations are introduced at this region's boundaries, in direct contradiction with the assumption of (global) independence. In other words, rectangular boundaries on our ABDS, CCB, and EWSB selection criteria, as imposed by the global assumption of statistical independence of randomly distributed variables, may provide an inaccurate probability estimate due to boundary effects in our selection criteria. However, it may still be reasonable to provide a rough, qualitative idea of the magnitude of stringy naturalness of a vacuum.

To address the normalization issue present with the measure P_μ, a clear choice arises from the problem being analyzed. Recall that we are searching for the relative abundance of ABDS-compliant vacua near some initial vacuum, relative to some total number of EWSB-compliant and no-CCB vacua near the same initial vacuum. In this sense, the set of EWSB-compliant and no-CCB vacua contains the set of ABDS-compliant vacua as a subset, since the ABDS-compliant vacua must also be compliant with EWSB and CCB conditions. Therefore, for some selection criteria represented as an indicator function $\theta(\text{criteria})$ and a joint probability density function $f(\vec{x})$ for a vector of random variables $\vec{x}$, a reasonable probability measure can be expressed as

$$P \sim \frac{\int \theta(\text{ABDS, EWSB, no CCB}) f(\vec{x})\, d\vec{x}}{\int \theta(\text{EWSB, no CCB}) f(\vec{x})\, d\vec{x}}. \tag{10}$$

Then, in keeping with the tradition of smaller naturalness values leading to greater levels of "naturalness", a clear choice for the stringy naturalness measure is

$$\Delta_{\text{SN}} = \frac{1}{P}. \tag{11}$$

Table 3.1 demonstrates the value of Δ_{SN} if $p\%$ of viable vacua satisfy the ABDS condition as well.

p (%)	Δ_{SN}
30	3.3
10	10
5	20
0.001	100000
10^{-25}	10^{27}

Table 1: Some approximate examples of the value of Δ_{SN} obtained if $p\%$ of EWSB-compliant and no-CCB vacua surrounding some initial vacuum with $m_Z = 91.2$ GeV are also ABDS-compliant.

By scanning the parameter space in one direction at a time, starting at the user-supplied vacuum, one can find "endpoints" in each direction of the parameter space, akin to the "width" of the ABDS window computed in the P_μ measure. In general, this collection of endpoints on our parameters creates an

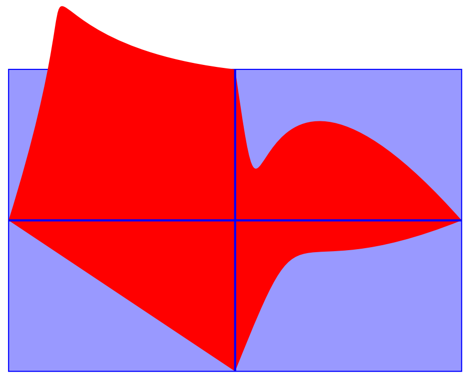

Figure 1: A 2D conceptual example showing the approximately bounding hyperrectangle (blue) mostly containing the desired subregion of the plane (red). The intersection of the vertical and horizontal dark blue lines represents the location of the user-submitted vacuum in this parameter space.

approximately bounding hyperrectangle in the space of random variables, approximately containing our subregion of interest. Consider the 2D example in Fig. 1 to illustrate this.

Fig. 1 demonstrates the idea that this method of computing independent probabilities is akin to computing the weighted area of the blue rectangle (weighted by the appropriate probability densities), whereas the "true" probability may be more like the weighted area of the red region. As such, since the blue region is usually at least as large as the red space, this could potentially overestimate the probability. The exception is when long "legs" of the red region leaving the blue bounding rectangle contribute significantly to the size of the red region as in Fig. 1, which may be less significant given an appropriate bounding rectangle or scanning regime. Moreover, the boundaries of the EWSB and no-CCB conditions are generally nonrectangular in this space. Hence, in Fig. 2, a more realistic demonstration of the general, nonrectangular shapes of boundaries for different selection criteria are pictured. Here, finding the probability of throwing a dart randomly at the Fig. 2 plane and hitting in the red region, normalized to the probability of hitting the blue region is conceptually similar to finding the number of ABDS-compliant vacua within neighboring EWSB-compliant and no-CCB vacua of the landscape. These approximation issues are addressed in the Monte-Carlo method, which will be discussed shortly.

Then, utilizing the probability density functions in Eqs. (8, 9) to count the relative abundance of ABDS-compliant vacua, we can write the following approximate expression for Δ_{SN}. Here, we denote the number of soft terms in our parameter space by n_{soft} (in practice, we will use $n_{\text{soft}} = 30$). We will denote the probability density of a random variable x with $f_x(x)$. The bounds of integration obtained from the one-dimensional initial scan over points satisfying EWSB and no-CCB conditions are generally denoted as $p_{i,\pm}$ and $\mu_{\pm}$, whereas the bounds of integration obtained from the one-dimensional initial scan over points satisfying EWSB and no-CCB conditions, along with being ABDS-compliant are generally denoted as $p_{i,\pm,A}$ and $\mu_{\pm,A}$, where A stands for "ABDS".

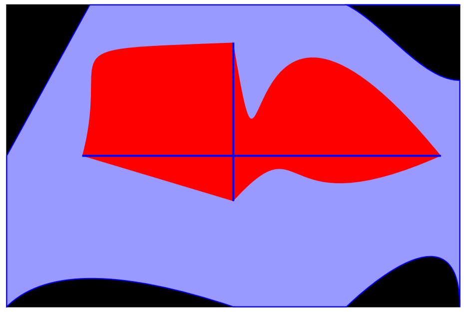

Figure 2: A 2D conceptual demonstration of regions of a parameter space containing EWSB-compliant and no-CCB vacua (blue) and vacua satisfying these criteria together with ABDS-compliance (red), in arbitrary, nonrectangular shapes. Regions in black are incompatible with EWSB or CCB conditions. Computing the probability of an event (a vacuum) in the red region is akin to the ratio of the areas of the red region to the blue region. This is most easily accomplished with Monte-Carlo sampling according to the distributions of the parameters. The intersection of the vertical and horizontal dark blue lines represents the location of the user-submitted vacuum in this parameter space.

$$\begin{aligned}
\Delta_{\mathrm{SN}} &= \prod_{i=1}^{n_{\mathrm{soft}}} \frac{\int \theta(\mathrm{EWSB},\ \mathrm{no\ CCB}) f_{p_i}(p_i)\ dp_i \int f_\mu(\mu)\ d\mu}{\int \theta(\mathrm{ABDS},\ \mathrm{EWSB},\ \mathrm{no\ CCB}) f_{p_i}(p_i)\ dp_i \int f_\mu(\mu)\ d\mu} \\
&\approx \prod_{i=1}^{n_{\mathrm{soft}}} \frac{\int\limits_{p_{i,-}}^{p_{i,+}} f_{p_i}(p_i)\ dp_i \int\limits_{\mu_-}^{\mu_+} f_\mu(\mu)\ d\mu}{\int\limits_{p_{i,-,A}}^{p_{i,+,A}} f_{p_i}(p_i)\ dp_i \int\limits_{\mu_{-,A}}^{\mu_{+,A}} f_\mu(\mu)\ d\mu} \\
&= \left[\prod_{i=1}^{n_{\mathrm{soft}}} \left(\frac{\int\limits_{p_{i,-}}^{p_{i,+}} p_i^{2n_F+n_D-1}\ dp_i}{\int\limits_{p_{i,-,A}}^{p_{i,+,A}} p_i^{2n_F+n_D-1}\ dp_i} \right)\right] \frac{\int\limits_{\mu_-}^{\mu_+} \frac{1}{\ln(10)|\mu|}\ d\mu}{\int\limits_{\mu_{-,A}}^{\mu_{+,A}} \frac{1}{\ln(10)|\mu|}\ d\mu} \\
&= \left[\prod_{i=1}^{n_{\mathrm{soft}}} \frac{\left[\left(p_{i,+}^{2n_F+n_D} - p_{i,-}^{2n_F+n_D}\right)\right]}{\left[\left(p_{i,+,A}^{2n_F+n_D} - p_{i,-,A}^{2n_F+n_D}\right)\right]}\right] \frac{\log\left(\frac{|\mu_+|}{|\mu_-|}\right)}{\log\left(\frac{|\mu_{+,A}|}{|\mu_{-,A}|}\right)} \geq 1
\end{aligned} \tag{12}$$

3.2 Numerical method for Δ_{SN}

In reality, the boundaries of the regions of selected vacua in the landscape parameter space are non-rectangular, so the integration bounds appearing in Eq. (12) are generally more complicated. There is a 30-dimensional surface enclosing a region in the 31-dimensional parameter space representing the boundary between vacua satisfying or violating the chosen selection criteria, and the integration bounds in a more precise evaluation of Δ_{SN} will generally be non-rectangular. Therefore, an explicit expression for Δ_{SN} in an $n = n_{\mathrm{soft}}$-dimensional parameter space would look more like the following:

$$\begin{aligned}
\Delta_{\mathrm{SN}} &= \frac{\int\int \theta(\text{EWSB, no CCB})\,[\prod_{i=1}^{n} f_{p_i}(p_i)]\, f_\mu(\mu)\; dp_i\; d\mu}{\int\int \theta(\text{ABDS, EWSB, no CCB})\,[\prod_{i=1}^{n} f_{p_i}(p_i)]\, f_\mu(\mu)\; dp_i\; d\mu} \\
&= \frac{\int_{\mu_-}^{\mu_+}\int_{p_{1,-}(\mu)}^{p_{1,+}(\mu)}\cdots\int_{p_{n,-}(\mu,p_1,\ldots,p_{n-1})}^{p_{n,+}(\mu,p_1,\ldots,p_{n-1})} [\prod_{i=1}^{n} f_{p_i}(p_i)]\, f_\mu(\mu)\; dp_n\ldots dp_1\; d\mu}{\int_{\mu_{-,A}}^{\mu_{+,A}}\int_{p_{1,-,A}(\mu)}^{p_{1,+,A}(\mu)}\cdots\int_{p_{n,-,A}(\mu,p_1,\ldots,p_{n-1})}^{p_{n,+,A}(\mu,p_1,\ldots,p_{n-1})} [\prod_{i=1}^{n} f_{p_i}(p_i)]\, f_\mu(\mu)\; dp_n\ldots dp_1\; d\mu} \\
&= \frac{\int_{\mu_-}^{\mu_+}\int_{p_{1,-}(\mu)}^{p_{1,+}(\mu)}\cdots\int_{p_{n,-}(\mu,p_1,\ldots,p_{n-1})}^{p_{n,+}(\mu,p_1,\ldots,p_{n-1})} [\prod_{i=1}^{n} |p_i|^{2n_F+n_D-1}]\, \frac{1}{|\mu|}\; dp_n\ldots dp_1\; d\mu}{\int_{\mu_{-,A}}^{\mu_{+,A}}\int_{p_{1,-,A}(\mu)}^{p_{1,+,A}(\mu)}\cdots\int_{p_{n,-,A}(\mu,p_1,\ldots,p_{n-1})}^{p_{n,+,A}(\mu,p_1,\ldots,p_{n-1})} [\prod_{i=1}^{n} |p_i|^{2n_F+n_D-1}]\, \frac{1}{|\mu|}\; dp_n\ldots dp_1\; d\mu}.
\end{aligned} \tag{13}$$

Expanding and solving an exact expression for this quickly becomes messy and complicated, if not impossible due to not knowing the exact location of the boundary *ab initio*. Briefly, the problem is in integrating in a high-dimensional space with only partially known bounds (recall that we know at least 62 points on the bounds–two boundary points in each direction of parameter space established previously). Such an expression would still need to be evaluated numerically, as the boundaries of the selection criteria region of the parameter space are generally unknown in structure.

Recall that the large dimension of this problem, such as in the MSSM parameter space, greatly exacerbates boundary effects seen in the bounds of the integrals above. Therefore, we have derived a method for efficiently approximating the integral in Δ_{SN} while obeying the correct bounds using a Monte Carlo integrator with a Monte Carlo semi-stratified importance sampler to select points for the integration. The idea is outlined in the bullet points below:

- We know one point within the region of desired integration: the user-submitted vacuum specified by an SLHA file.

- Akin to the hyperrectangle formulation of Eq. (12), we can find one-dimensional boundaries to our integration region, relative to our initial point. We save these one-dimensional bounds for future use.

- We partition the 31-dimensional parameter space into two-dimensional slices containing the "origin" (the original SLHA-supplied vacuum). There are $\binom{31}{2} = 465$ such slices, and each of these slices are bounded in each perpendicular direction by the respective one-dimensional bounds of that slice, obtained previously. We then sample from the appropriate distributions within these slices or within the whole parameter space to refine the Monte Carlo integration estimate of Δ_{SN}.

  – In practice, for some points of the Monte Carlo integration routine, we start by randomly sampling two integers uniformly between 1 and 31, including these endpoints. These will index two of the 31 parameters in our space, allowing us to select a random two-dimensional slice of our large parameter space. From this random slice, a planar region exists that is bounded by the individual one-dimensional limits obtained from the user-submitted file and contains the user-supplied vacuum. This two-dimensional region then can be sampled uniformly to find a new vacuum to test for inclusion in the Monte Carlo integrator. If the relevant conditions are satisfied (EWSB, CCB, and/or ABDS), then the value is added into the Monte Carlo integrator – otherwise, the Monte Carlo integrator effectively adapts the integration region, refining it according to this conditional failure.

  – The sampled region contains the original vacuum by construction and approximately contains the desired region of integration within the random slice.

- This process is iterated until some specified level of convergence in the integral is reached.

We perform this integration with a Monte Carlo integration technique using a "semi-stratified" importance sampling mechanism, where semi-stratified refers to an alternation between sampling the entire parameter space and sampling slices, as described above. In practice, this means we sample points from each of the slices of our parameter space according to the probability densities of the points in these planes, which are easily computable since the parameters are independently distributed with known densities. Since the sampling distribution matches the integrand we are approximating the integral of, this is an example of ideal importance sampling, or self-normalized importance sampling. The integral approximation for a scalar-valued vector function $f_S(\vec{x})$ over a region S contained in a larger region R involves N sample points $\vec{x}_1, \ldots, \vec{x}_N$, each drawn from R with the selection distribution $f(\vec{x})$. But the target probability density $f_S(\vec{x})$ simply consists of a probability density function very similar to $f(\vec{x})$ (these are *unnormalized* probability densities – recall the normalization comes from how we constructed $\Delta_{\rm SN}$) convolved with a binary indicator function θ indicating the region S within R. With this nearly optimal choice in selection distribution, the integral is approximated as

$$\begin{aligned} I = \int_S f_S(\vec{x})\, d\vec{x} &\approx \frac{1}{N}\sum_{i=1}^{N} \frac{f_S(\vec{x}_i)}{f(\vec{x}_i)} \\ &\approx \frac{1}{N}\sum_{i=1}^{N} \left(\begin{cases} 1 & \text{if } \vec{x}_i \in S \\ 0 & \text{otherwise} \end{cases} \right) \\ &= \frac{n_S}{N}. \end{aligned} \tag{14}$$

In other words, with this choice of Monte Carlo integrator, we can approximate the integral of the joint probability function in Eq. (13) as a the number of vacua n_S satisfying the conditions of θ, divided by the total number of vacua, N, scanned in the scanning region. This is in alignment with the definition of stringy naturalness we began with, so this lends credence to this selection of a Monte Carlo integrator while simultaneously approximately minimizing the variance of our approximation.

Thus, using this careful Monte Carlo simulation and integrator, we approximate $\Delta_{\rm SN}$ more rigorously than in Eq. (12) as

$$\begin{aligned} \Delta_{\rm SN} &\approx \frac{\frac{n_{\theta,\rm tot}}{N_{\rm tot}}}{\frac{n_{\theta,A}}{N_A}} \\ &= \frac{n_{\theta,\rm tot} N_A}{n_{\theta,A} N_{\rm tot}}, \end{aligned} \tag{15}$$

where $N_{\rm tot}$ is the total number of vacua scanned in the whole bounding hyperrectangle, $n_{\theta,\rm tot}$ is the number of vacua scanned in $N_{\rm tot}$ satisfying at least EWSB and no-CCB conditions, $N_{\rm A}$ is the total number of vacua scanned in a smaller hyperrectangle approximately bounding the ABDS region, and $n_{\theta,A}$ is the number of vacua scanned in $N_{\rm A}$ satisfying EWSB, no-CCB, and ABDS conditions. If $N_A = N_{\rm tot}$ (i.e., one single copy of this Monte Carlo integrator tries to account for both integrals in Eq. (13) simultaneously), the expression above simplifies, but $n_{\theta,A}$ may not be adequately represented due to undersampling of this region. Therefore, it is best to have *two* Monte Carlo integrators handling the two sets of integrals in Eq. (13) running together, since $n_{\theta,A}$ and N_A can contribute to $n_{\theta,\rm tot}$ and $N_{\rm tot}$.

To assist with stability of the Monte Carlo integrator's convergence on a solution, as well as protecting its sensitivity to outliers in the limit of large N, a smooth relative error cutoff is used involving a simple moving average of the integral approximation across the iterations $\{N-k, N-k+1, \ldots, N-1, N\}$, where this moving average is represented by the function $M(I_{N-k}, \ldots, I_N, k)$:

$$\epsilon > \frac{|M(I_{N-k}, \ldots, I_{N-1}, I_N, k) - I_N|}{I_N}. \tag{16}$$

This condition determines the convergence and termination of the iterative approximation. Good choices for ϵ may be $\epsilon = 10^{-3}$ or $\epsilon = 10^{-6}$. Smaller values of epsilon would require a (potentially significantly) greater number of sample points N for an accurate evaluation. In practice, we take $k = 100$ to ensure adequate smoothing of data based on empirical observation obtained during the simulation.

3.3 Yukawa and gauge couplings

Note that so far, nothing has been mentioned regarding Yukawa and gauge couplings in our systematic landscape scans. One might naïvely think that the Yukawas and gauge couplings could be held invariant between different vacua at the GUT scale. However, since the MSSM parameter b is considered fundamental in regards to the soft parameter distributions, b is no longer a free parameter to be solved for from the second Higgs minimization condition, Eq. (4). Instead b(weak) is fixed by its GUT scale value and corresponding RGE running, meaning β must no longer be fixed for consistency, but instead must be solved for on a point-by-point basis along with m_Z. Thus, part of the routine in checking the conditions in θ entails finding a simultaneous solution (m_Z, β) to Eqs. (3, 4).

This altered value of β from vacuum to vacuum can potentially significantly alter the distribution of the Yukawa couplings and even the gauge couplings through RGE running and a vacuum-dependent Higgs VEV. This is addressed in Requirement 3(d) of Section 2 by carefully using a Yukawa coupling boundary condition routine to fix the Standard Model masses to their known values and extract Yukawa couplings. Simultaneously, a gauge coupling boundary condition routine fixes the known Standard Model $\overline{\text{MS}}$ values of the electromagnetic and strong couplings. These can be converted to the appropriate scheme, corrected with threshold corrections, and found for the vacuum in question during the scan. This effectively constrains us to vacua where the Standard Model's fermion masses and gauge couplings are achievable at low energies, but possibly with a large Z boson mass. Of particular note is that this numerical effect of the statistics of μ and the soft parameters presented here induces some intrinsic distributions on β, m_Z, the Yukawa couplings, and the gauge couplings through RGE running and minimization conditions, which should be analyzed thoroughly in a later work.

4 An algorithm for stringy naturalness from SLHA outputs

Below is a series of flowcharts demonstrating the algorithm, code-named DSN4SLHA, presented here. For formatting purposes, the algorithm has been split into three flowcharts below. The full flowchart may be seen in the README file at https://github.com/Dmartinez-96/DSN4SLHA.

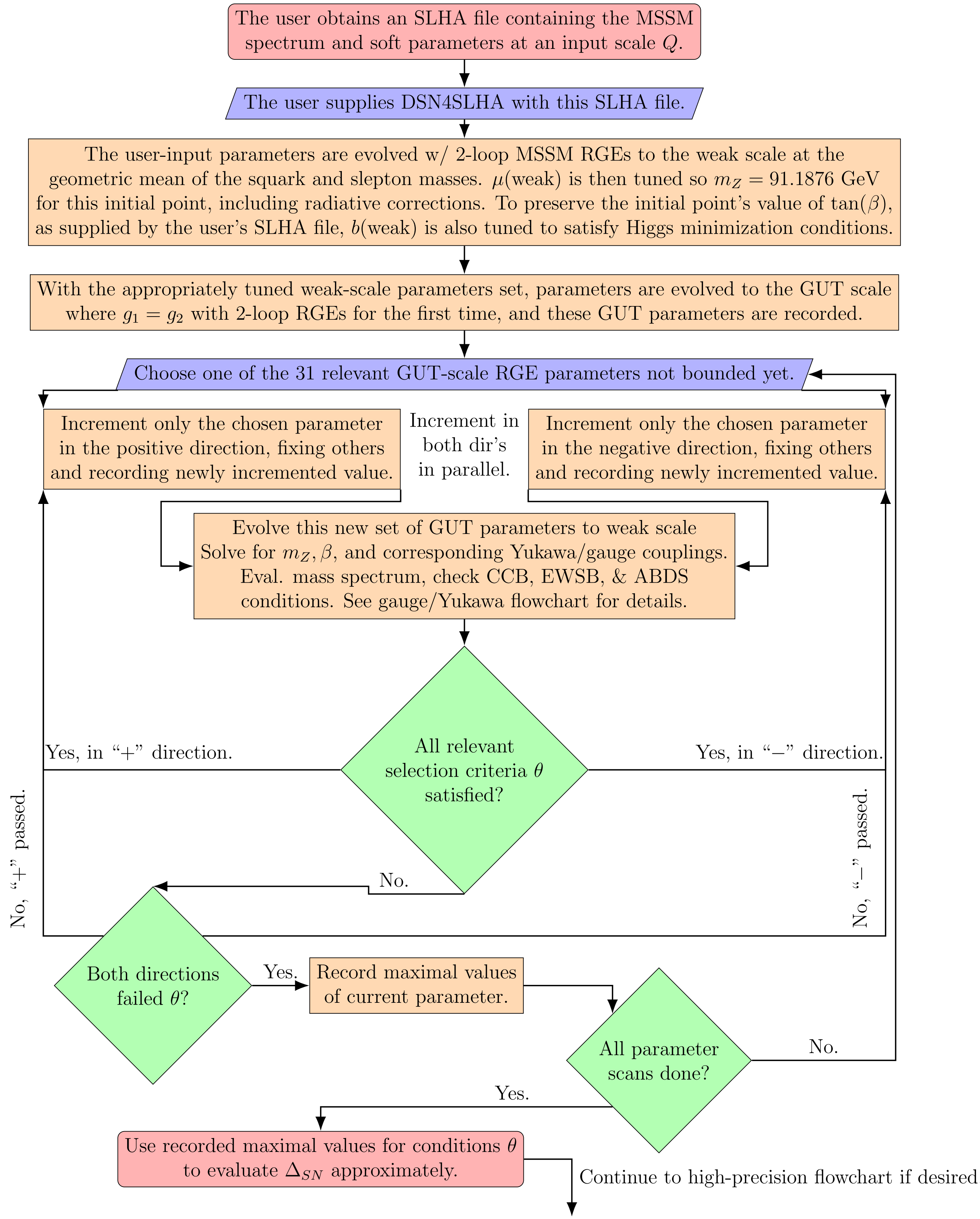

Figure 3: A flowchart describing the approximate, P_μ-esque derivation of Δ_{SN} as in Eq. (12).

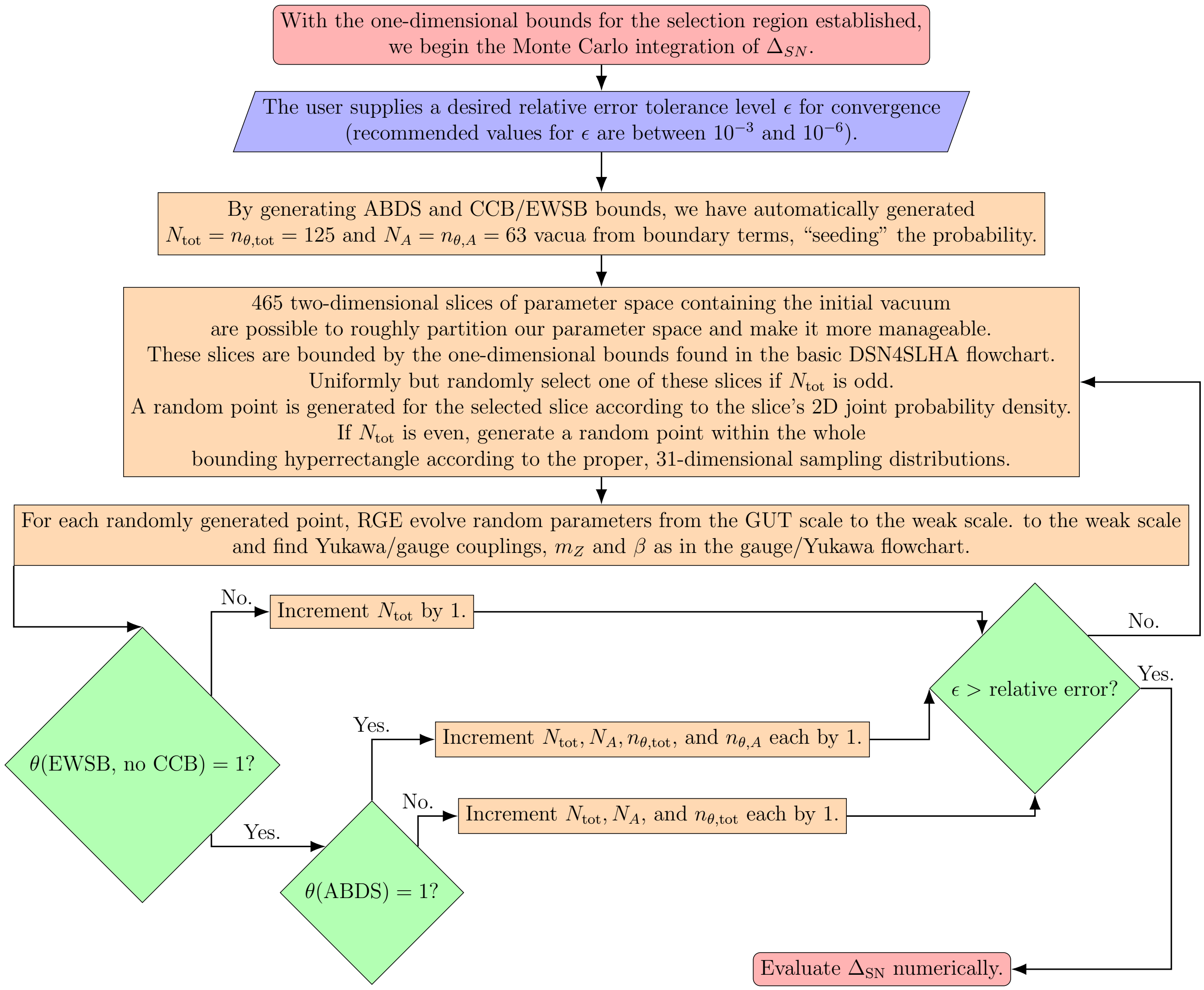

Figure 4: A flowchart describing the Monte Carlo integration of Eq. (13) by Monte Carlo integration with stratified importance sampling to approximate Δ_{SN} as Eq. (15). This method is amenable to parallelization, adding the results for the n's and N's from independent Monte Carlo integrators running in parallel to speed up computations. A combination of stratified importance sampling from the 2D slices with full-space importance sampling helps adequately cover this high-dimensional space.

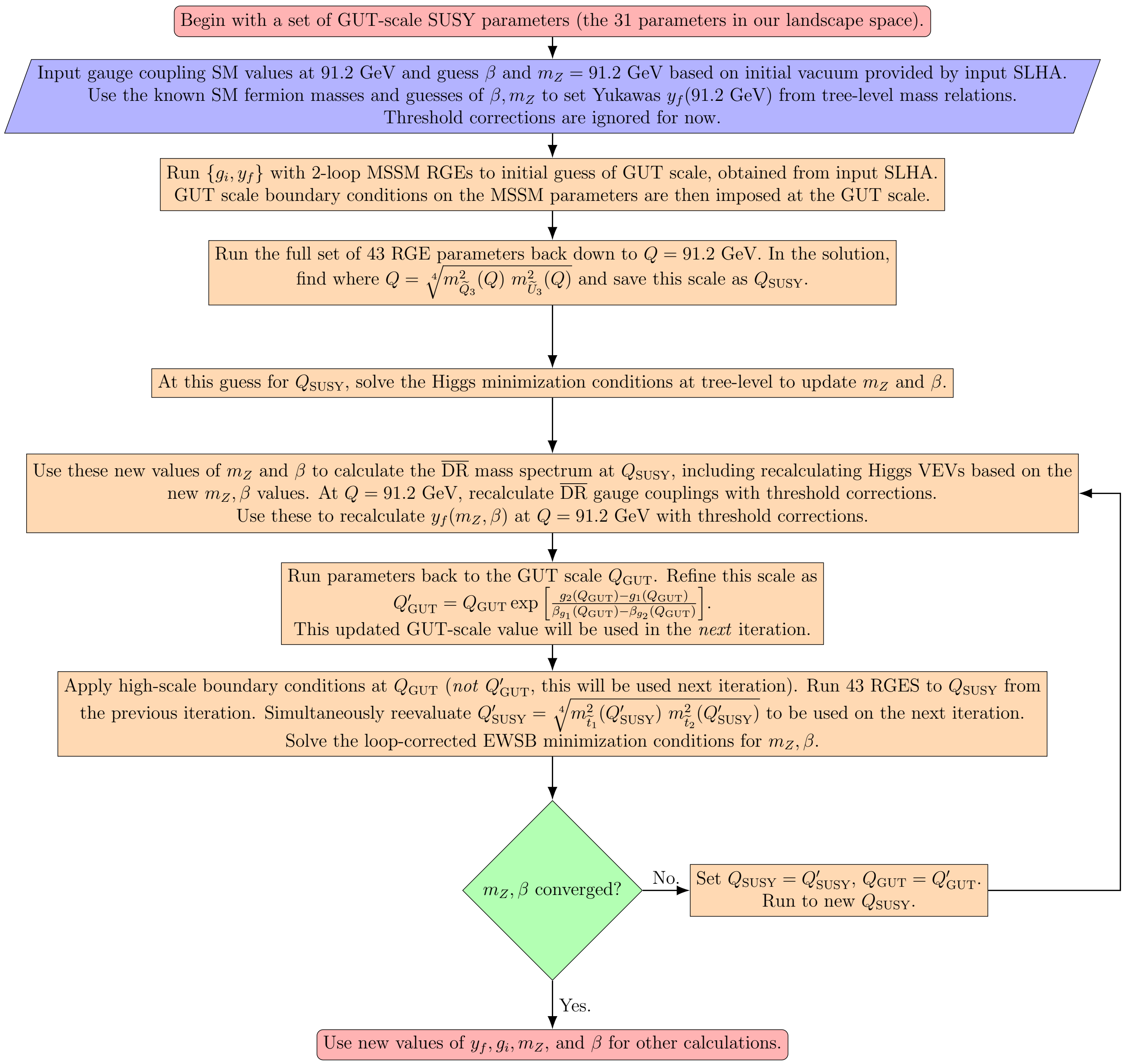

Figure 5: A flowchart describing the routine for establishing gauge and Yukawa coupling values based on known Standard Model masses in a given MSSM vacuum.

References

[1] H. Baer, V. Barger, S. Salam, Naturalness versus stringy naturalness with implications for collider and dark matter searches, Physical Review Research 1 (2) (9 2019). doi:10.1103/physrevresearch.1.023001.

[2] H. Baer, V. Barger, D. Martinez, S. Salam, Radiative natural supersymmetry emergent from the string landscape, Journal of High Energy Physics 2022 (3) (3 2022). doi:10.1007/jhep03(2022)186.

[3] M. R. Douglas, Statistical analysis of the supersymmetry breaking scale (6 2004). arXiv:0405279v4, doi:10.48550/arXiv.hep-th/0405279.

[4] P. Skands, B. Allanach, H. Baer, C. Balazs, G. Belanger, F. Boudjema, A. Djouadi, R. Godbole, J. Guasch, S. Heinemeyer, W. Kilian, J.-L. Kneur, S. Kraml, F. Moortgat, S. Moretti, M. Muhlleitner, W. Porod, A. Pukhov, P. Richardson, S. Schumann, P. Slavich, M. Spira, G. Weiglein, SUSY les houches accord: Interfacing SUSY spectrum calculators, decay packages, and event generators, Journal of High Energy Physics 2004 (07) (2004) 036–036. doi:10.1088/1126-6708/2004/07/036.

[5] B. Allanach, C. Balázs, G. Bélanger, M. Bernhardt, F. Boudjema, D. Choudhury, K. Desch, U. Ellwanger, P. Gambino, R. Godbole, T. Goto, J. Guasch, M. Guchait, T. Hahn, S. Heinemeyer, C. Hugonie, T. Hurth, S. Kraml, S. Kreiss, J. Lykken, F. Moortgat, S. Moretti, S. Peñaranda, T. Plehn, W. Porod, A. Pukhov, P. Richardson, M. Schumacher, L. Silvestrini, P. Skands, P. Slavich, M. Spira, G. Weiglein, P. Wienemann, SUSY les houches accord 2, Computer Physics Communications 180 (1) (2009) 8–25. doi:10.1016/j.cpc.2008.08.004.

[6] H. Baer, V. Barger, D. Martinez, Comparison of SUSY spectra generators for natural SUSY and string landscape predictions, The European Physical Journal C 82 (2) (2 2022). doi:10.1140/epjc/s10052-022-10141-2.